

## Influence of Polymer Molecular Weight on the Chemical Modifications Induced by UV Laser Ablation

Esther Rebollar,<sup>†</sup> Giannis Bounos,<sup>‡</sup> Mohamed Oujja,<sup>†</sup> Concepción Domingo,<sup>§</sup>  
Savas Georgiou,<sup>‡</sup> and Marta Castillejo<sup>\*,†</sup>

*Institute of Physical Chemistry Rocasolano, CSIC, Serrano 119, 28006 Madrid, Spain, Foundation for Research and Technology—Hellas, Institute of Electronic Structure and Laser, P.O. Box 1527, 71110 Heraklion, Crete, Greece, and Instituto de Estructura de la Materia, CSIC, Serrano 121, 28006 Madrid, Spain*

*Received: March 9, 2006; In Final Form: May 29, 2006*

This paper investigates the influence of polymer molecular weight ( $M_w$ ) on the chemical modifications of poly(methyl methacrylate), PMMA, and polystyrene, PS, films doped with idonaphthalene (NapI) and iodophenanthrene (PhenI), following irradiation at 248 nm (KrF excimer laser, 20 ns fwhm and hybrid excimer-dye laser, 500 fs fwhm) and at 308 nm (XeCl excimer laser, 30 ns fwhm). The changes of intensity and position of the polymer Raman bands upon irradiation provide information on cleavage of the polymer bonds. Degradation of PMMA, which is a weak absorbing system at 248 nm, occurs to a higher extent in the case of a larger  $M_w$ , giving rise to the creation of unsaturation centers and to degradation products. For highly absorbing PS, no degradation is observed upon irradiation with a KrF laser. Consistently irradiating doped PS at 308 nm, where the absorption is low, induces degradation of the polymer. Results provide direct support for the bulk photothermal model, according to which ejection requires a critical number of broken bonds. In the case of irradiation of doped PMMA with pulses of 248 nm and 500 fs, neither degradation nor dependence with polymer  $M_w$  are observed, indicating that mechanisms involved in the femtosecond laser ablation differ from those operating in the case of nanosecond laser ablation. Participation of multiphoton/avalanche processes is proposed.

### Introduction

Because of the increasing importance of UV ablation for the analysis and processing of molecular substrates (e.g., in microelectronics, medicine, art conservation, etc.), substantial effort has been directed toward elucidation of the processes underlying it. In this framework, a wide range of studies<sup>1–4</sup> on the dependence of the phenomenon on laser irradiation and material parameters has been reported. Particular emphasis has been placed on the importance of wavelength since the use of short wavelengths has been considered to promote a photochemical mechanism at the expense of a photothermal one, with a consequent improvement of the morphology of the processed area. A wide range of different polymers has also been examined to elucidate the influence of chemical composition on the efficiency and mechanism of ablation.<sup>5</sup> More recently, femtosecond (fs) irradiation has resulted in powerful, new material processing capabilities.<sup>6,7</sup> It is generally demonstrated that the quality of structuring with femtosecond pulses far surpasses that attained in nanosecond (ns) ablation.<sup>8</sup>

Surprisingly, very little work has been reported on the influence of the polymer molecular weight ( $M_w$ ) on the ablation process,<sup>9–14</sup> despite the fact that this parameter determines crucially most polymer physical properties such as transition temperatures and mechanical properties. Furthermore, in several

applications, especially medical and art conservation applications, the  $M_w$  of the treated polymer-like substrates may vary considerably from case to case. In all, both for mechanistic purposes and for the interest of applications, it is important to characterize the influence of polymer  $M_w$  on the laser ablation process.

Lemoine et al.<sup>9</sup> studied the effect of  $M_w$  on the 248 nm photoablation of polystyrene, PS, and Lippert et al.<sup>10</sup> studied the influence of the degree of polymerization on the ablation of poly(methyl methacrylate), PMMA, at 308 nm. Mito et al.<sup>11</sup> have examined the temporal dynamics of the morphological changes of PS of different  $M_w$  via time-resolved interferometry. They have shown that the time scale of expansion and especially of contraction of films upon laser irradiation changes for different  $M_w$  systems. All the previously stated studies have focused on physical processes and have not examined any plausible dependence for the chemical ones.

Vibrational spectroscopy techniques have been previously used for the characterization of the effects of laser irradiation of polymers. Beauvois et al. used FTIR spectroscopy to study the cross-linking process that takes place in PMMA upon irradiation at 248 nm.<sup>15</sup> Küper and Stuke also employed FTIR spectroscopy after irradiation of PMMA at 248 nm, and the results revealed the presence of the bonds C=C and C≡C, the latter due to occluded carbon monoxide.<sup>16</sup> Rossier et al. employed microconfocal Raman spectroscopy for crystallinity measurements of polyethyleneterephthalate, PET, before and after laser irradiation at 193 nm.<sup>17</sup> Lippert et al. used Raman spectroscopy to study the effects of laser ablation of polyimide, PI, at different wavelengths.<sup>18,19</sup> In their studies, Raman spectra

\* Corresponding author. Tel.: +34-915619400; fax: +34-915642431; e-mail: marta.castillejo@iqfr.csic.es.

<sup>†</sup> Institute of Physical Chemistry Rocasolano.

<sup>‡</sup> Institute of Electronic Structure and Laser.

<sup>§</sup> Instituto de Estructura de la Materia.

were used to confirm that carbonization occurs. Micro-Raman studies carried out by Lazare et al. after irradiation at 248 nm of PMMA showed formation of conjugated structures ( $\text{C}=\text{C}-\text{C}=\text{C}$  units), and isolated  $\text{C}=\text{C}$  units<sup>20</sup> originated from photolysis of the ester side chain.

Recently,<sup>12–14</sup> we have shown initial results of the decisive influence of  $M_w$  on the morphological and chemical modifications induced in films of PMMA and PS doped with the iodo derivatives of the aromatics naphthalene (NapI) and phenanthrene (PhenI). In this paper, we present a more comprehensive study on the effect of  $M_w$  on the chemical modifications induced by UV laser ablation of those systems via Raman microscopy. Films of PMMA and PS, of an average  $M_w$  in the range of 2–1000 kDa, were irradiated in air by a KrF excimer laser (248 nm, 20 ns fwhm), a XeCl excimer laser (308 nm, 30 ns fwhm) in the case of PS based systems, and a hybrid excimer-dye laser (248 nm, 500 fs fwhm). The results reported here show that laser irradiation induces degradation of the polymer and that this occurs to a higher extent in larger  $M_w$  polymers for low absorbing systems. Instead, for PS, which strongly absorbs at 248 nm, no degradation is observed. On the other hand, chemical modifications are observed for PS irradiation/ablation at the weakly absorbed wavelength of 308 nm, very much similar to PMMA. Results are analyzed within the framework of the bulk photothermal model,<sup>21,22</sup> according to which ejection requires a critical number of bonds to be broken.

In the case of irradiation with a hybrid excimer-dye laser with a pulse duration of 500 fs, neither degradation nor dependence on polymer  $M_w$  is observed. Mechanisms involved in the femtosecond laser ablation differ from those that operate in the case of nanosecond laser ablation. Results obtained for femtosecond laser ablation should enable the successful processing of a wide range of substrates as those found in restoration of artwork or for biological applications since their success is related to highly restricted and selective chemistry.

## Experimental Procedures

Highly purified PMMA with average  $M_w$  of 2.5 kDa (Polymer Standard Service) and 120 and 996 kDa (Aldrich) and PS average  $M_w$  of 15.1 kDa (Polymer Standard Service), 280 kDa (Aldrich), and 532 kDa (Polymer Standard Service) were doped with iodonaphthalene (NapI) and iodophenanthrene (PhenI) (Aldrich). The films were prepared by casting solutions of the purified polymer and of the dopant dissolved into dichloromethane ( $\text{CH}_2\text{Cl}_2$ ) on quartz substrates. The dopant concentration varied from 0.5 to 1.2 wt %, and the typical film thickness was in the range of 20–100  $\mu\text{m}$ , as measured by a DEKTAK 3030 profilometer. Doping of the polymers resulted in an increase of absorption coefficient that, however, is not dependent on the polymer  $M_w$  as established by direct transmission studies.<sup>12,13</sup>

The targets were irradiated by a KrF excimer laser (248 nm, 20 ns fwhm) focused at normal incidence and by a hybrid excimer-dye laser (248 nm, 500 fs fwhm) at fluences up to 2000 and 700  $\text{mJ}/\text{cm}^2$ , respectively, to explore the effects of irradiation below and above the swelling onset and the etching threshold of the samples<sup>13</sup> shown in Table 1. PS films were also irradiated by a XeCl laser (308 nm, 30 ns fwhm) at fluences up to 3900  $\text{mJ}/\text{cm}^2$ . The Raman spectra were recorded with a Renishaw Raman microscope system RM1000 coupled to an optical Leica DM LM microscope. The Raman system was equipped with an electrically refrigerated CCD camera and a diode laser at 785 nm as the excitation source, operating at a power level of 30 mW. The spectra were acquired by collecting scattered light

**TABLE 1: Optical Penetration Depth as Determined from Effective Absorption Coefficient, Swelling Onset, and Ablation Threshold (in  $\text{mJ}/\text{cm}^2$ , Errors Estimated To Be 10–20%) of Doped Polymer Films upon Irradiation with KrF Laser (248 nm, 20 ns fwhm)**

	$M_w$ (kDa)	optical penetration depth ( $\mu\text{m}$ )	swelling	ablation
1.2% NapI/PMMA	2.5		250	1100
	120	6	600	1500
	996		650	1500
1.2% PhenI/PMMA	2.5		180	540
	120	4	180	800
	996		180	800
0.5% PhenI/PS	15.1		<i>a</i>	
	280	0.3	<i>a</i>	50
	532		<i>a</i>	

<sup>a</sup>Not observable.

from the surface in backscattering geometry. The diameter of the laser spot on the sample was diffraction limited by the objective lens ( $0.61\lambda/\text{NA}$ , with  $\lambda = 785$  nm and NA the numerical aperture of the lens) and calculated to be  $\sim 1$   $\mu\text{m}$ . The depth of the Raman probe was 2  $\mu\text{m}$ . The spectra were taken with a spectral resolution of 4  $\text{cm}^{-1}$  and exposure times in the range of 10–60 s, the final spectra resulting from the accumulation of five individual ones.

For a comparison between the intensity of the bands in nonirradiated and irradiated areas, the intensity of every band was normalized to that at 600  $\text{cm}^{-1}$  assigned to the stretching mode ( $\nu_s$ ) of ( $\text{C}-\text{C}-\text{O}$ ). This band was selected because it corresponds to the vibration of the bond between the backbone and the side chain of the polymer (see inset in Figure 1).

## Results

Analyses of the Raman spectra are illustrated here for the PhenI-doped samples. Samples doped with NapI were also analyzed, yielding similar results. Relevant parts of the Raman spectra of PhenI-doped PMMA films of  $M_w$  of 996 kDa are shown in Figure 1. The two bands at 736 and 1125  $\text{cm}^{-1}$  are readily assigned to the  $\nu(\text{C}-\text{C})$  skeletal mode of PMMA.<sup>23</sup> Bands at 370, 484, 600, 818, 1234, and 1736  $\text{cm}^{-1}$  are associated with the  $\text{C}-\text{COOCH}_3$  group.<sup>23</sup> In particular, the 1736  $\text{cm}^{-1}$  band corresponds to the stretching mode of  $\text{C}=\text{O}$  in the ester carbonyl group. Other bands are assigned to an  $\text{O}-\text{CH}_3$  rock at 990  $\text{cm}^{-1}$ ,  $\text{C}-\text{H}$  bending at 1460  $\text{cm}^{-1}$ , and  $\text{C}-\text{H}$  stretching vibrations of  $\text{CH}_2$  and  $\text{CH}_3$  at 3100–2800  $\text{cm}^{-1}$  (not shown in the figure). Bands of the dopants also contribute to the Raman spectra, as the one observed at 1345  $\text{cm}^{-1}$  due to PhenI (1367  $\text{cm}^{-1}$  in the case of NapI).

**Nanosecond Irradiation.** Table 1 shows the swelling onsets and ablation thresholds determined by profilometric measurements at 248 nm of the studied polymer films. The optical penetration depths also listed in the table were calculated from the effective absorption coefficients determined from measurements below the ablation threshold. Upon irradiation of PMMA at this weakly absorbed wavelength, the swelling onsets and the etching thresholds increase with increasing  $M_w$ . However, for doped PS, which strongly absorbs at 248 nm, the ablation thresholds are not dependent on  $M_w$ . In the PMMA based systems, the etch depth per pulse (at 248 nm) reaches up to 10  $\mu\text{m}$  at the highest fluences used; in doped PS, the stronger optical absorption reduces significantly the etch depth. In addition to swelling and etching, irradiation of the films induces morphological modifications in the form of bubbles.<sup>14</sup> In all PMMA based samples, the thickness of the modified layer is smaller

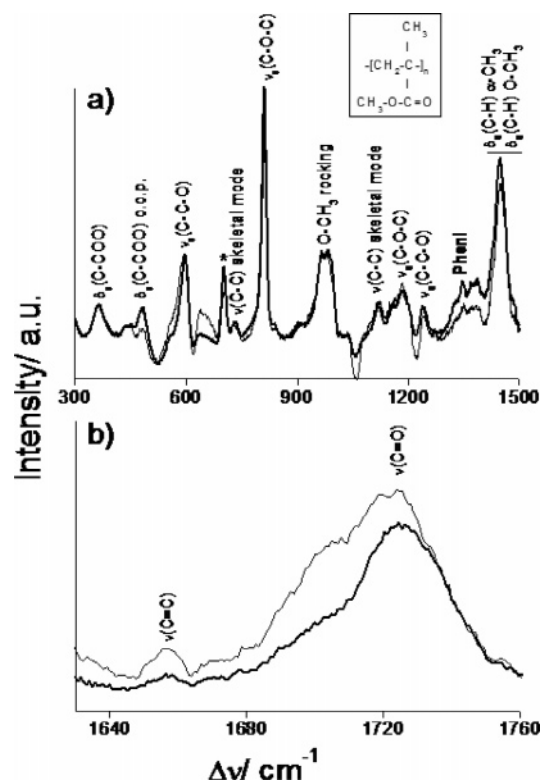


**Figure 1.** Micro-Raman spectra of films of 1.2 wt % PhenI doped PMMA with a  $M_w$  of 996 kDa. The two spectra shown were taken with a spectral resolution of  $4\text{ cm}^{-1}$ , exposure time of 60 s, and accumulation of five successive individual ones. Unexposed and irradiated areas (1 KrF pulse at  $1030\text{ mJ/cm}^2$ ) are represented by thick and thin solid lines, respectively. The band marked with an asterisk is due to traces of the solvent dichloromethane. Chemical structure of PMMA is shown in the inset.

**TABLE 2: Main Effects Observed in Irradiated Areas of 1.2% PhenI/PMMA upon Irradiation at 248 nm**

Raman band	1.2% PhenI/PMMA 2.5 kDa <sup>a</sup>	1.2% PhenI/PMMA 996 kDa <sup>a</sup>
$\nu(\text{C}=\text{C})$	1 pulse 110 mJ/cm <sup>2</sup> , $\gamma = 1.3$ 1 pulse 1030 mJ/cm <sup>2</sup> , $\gamma = 1.5$	1 pulse 110 mJ/cm <sup>2</sup> , $\gamma = 6.1$ 1 pulse 1030 mJ/cm <sup>2</sup> , $\gamma = 9.2$
$\nu(\text{C}=\text{O})$	new bands	new bands
$\nu_s(\text{C}-\text{C}-\text{O})$	shifts to 595 cm <sup>-1</sup>	shifts to 595 cm <sup>-1</sup>

<sup>a</sup> $\gamma$  is defined as the ratio  $I_{\text{irradiated}}/I_{\text{virgin}}$  where  $I_{\text{irradiated}}$  and  $I_{\text{virgin}}$  are the intensity of the band in the irradiated area and in a nonirradiated area, respectively.

than the initial film thickness and larger (or comparable) than the Raman probe depth.

Upon irradiation at 248 nm of 1.2% PhenI/PMMA systems with a fluence of 110 mJ/cm<sup>2</sup>, below the corresponding ablation thresholds, a band at 1640 cm<sup>-1</sup> is observed in the spectra that can be ascribed to the stretching mode of the C=C bond. This band is associated with the end-groups of oligomer chains or with the presence of methyl methacrylate monomer (MMA).<sup>24</sup> Most importantly, the intensity of this band is considerably higher for the high  $M_W$  system as shown in Table 2. The growth of the ratio  $\gamma$  of the intensities of the band at 1640 cm<sup>-1</sup> in the irradiated and virgin polymer ( $\gamma = I_{\text{irradiated}}/I_{\text{virgin}}$ ) is higher for the higher  $M_W$  polymer. This ratio increases by a factor of 1.3 for a  $M_W$  of 2.5 kDa versus a factor of 6.1 for a  $M_W$  of 996 kDa (Table 2). Another effect observed is that the band that corresponds to  $\nu(\text{C}-\text{C}-\text{O})$  shifts from 600 to 595 cm<sup>-1</sup>.

Upon ablation, the morphology of the films is modified,<sup>14</sup>

thereby resulting in different scattering of the probe beam, thus affecting the quantification of the Raman signals. In Figure 1, the spectra, as indicated previously, have been normalized to the same band at  $600\text{ cm}^{-1}$ , and the subsequent discussion is limited to the spectral changes and major band intensity changes.

In the irradiation of 1.2% PhenI/PMMA at 1030 mJ/cm<sup>2</sup> (well above the ablation threshold, Table 1), the same effects as those at lower fluences are observed but to a higher extent, and differences between low and high  $M_w$  are more pronounced, as shown in Table 2. The intensity of the band corresponding to the C=C bond at 1640 cm<sup>-1</sup> increases considerably, the ratio  $\gamma$  for  $\nu_s$  (C=C) increases by a factor of 1.5 for the low  $M_w$  and by a factor of 9.2 for the high  $M_w$ . In parallel, new bands/shoulders are detected in the region of 1700–1800 cm<sup>-1</sup>, corresponding to the stretching mode of C=O (Figure 1b). These new bands can be assigned to degradation products formed upon UV irradiation. Possible products include aldehydes, carboxylic acids, and esters (monomers). In fact, characteristic bands of aldehydes appear in the region 1720–1740 cm<sup>-1</sup>, and the bands corresponding to carboxylic acids<sup>25</sup> appear at 1700–1740 cm<sup>-1</sup>. Methacrylates also have their typical bands<sup>25</sup> at 1710–1725 cm<sup>-1</sup>. In all, although the observed Raman bands in the region 1700–1800 cm<sup>-1</sup> cannot unambiguously specify the compounds, they can be ascribed to degradation products that remain in the substrate upon laser irradiation. Most importantly, the degradation is more extensive for the higher  $M_w$ .

When irradiating with 10 pulses at fluences below and above the ablation threshold, degradation occurs again at a higher extent in the high  $M_w$  polymer, but there is not a significant increase of the ratio  $\gamma$  in comparison to the effects induced upon irradiation with one single pulse. This most likely indicates that the changes within the depth probed by Raman microscopy have been saturated or that products from this depth diffuse out and desorb upon irradiation with successive pulses, thus preventing their buildup in the substrate.

The intensity of the band at  $1345\text{ cm}^{-1}$ , assigned to the dopant PhenI, decreases upon irradiation. This effect is observed for both the low and the high  $M_w$ . The decrease of this band is indicative of the decomposition of the dopant. Iodoaromatics, ArI (PhenI and NapI), are characterized by simple reactivity patterns. These compounds undergo a simple homolytic photodissociation to aryl (Ar) and halogen radicals.<sup>26–34</sup> The Ar radicals react via hydrogen-atom abstraction from the polymer to form ArH. The Raman spectrum of PhenH presents a band in the same region as the one assigned here to PhenI; thus, the intensity of this band should remain constant if only the decomposition of PhenI and formation of PhenH were taking place. Consequently, the decrease of the band at  $1345\text{ cm}^{-1}$  is mainly due to material being removed from the substrate by the etching process as shown elsewhere.<sup>30,35</sup>

In the case of doped PS, upon irradiation with a KrF laser, even at fluences well above the ablation threshold, the spectra corresponding to irradiated areas are not significantly different from those of the virgin substrate. This may suggest that minimal degradation of the polymer occurs. However, the thickness of the affected layer is too small to be adequately measured by the Raman probe. In contrast, irradiation with a XeCl laser at 308 nm, at which PS absorbs weakly, induces a decrease in the intensity of all the bands, as shown in Figure 2. Still, this observation is in good agreement with the results obtained by other techniques.<sup>13,14</sup> In fact, at 248 nm, no particular morphological changes can be detected in the optical microscopic examination, with the irradiated region appearing smooth. In contrast, similarly to what is observed in PMMA at



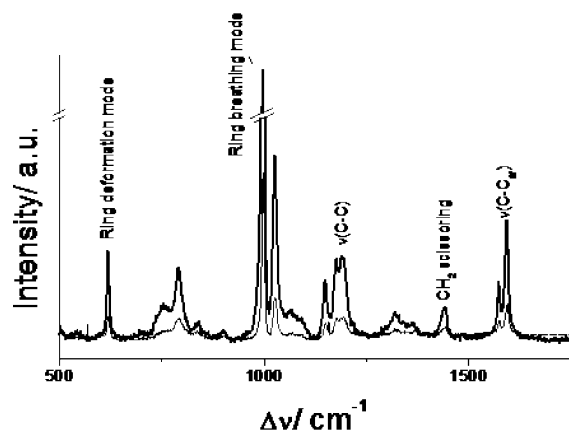


**Figure 2.** Micro-Raman spectra of films of 0.5 wt % PhenI doped PS with a  $M_w$  of 15.1 kDa. The spectra shown were taken with a spectral resolution of  $4\text{ cm}^{-1}$ , exposure time of 60 s, and accumulation of five successive individual ones. Unexposed and irradiated areas (1 XeCl pulse at  $3870\text{ mJ/cm}^2$ ) are represented by thick and thin solid lines, respectively.

248, the irradiated substrates of doped PS at 308 nm display morphological modifications of micrometric size. The optical absorption coefficient of pure PS at 248 nm is 30 times higher than the corresponding coefficient of pure PMMA ( $2740\text{ vs }90\text{ cm}^{-1}$ ), and the absorption coefficients increase for the doped polymers.<sup>13</sup> In this case, material removal occurs efficiently, with minimal heat diffusion and light penetration to the remaining substrate. This argument has been used to account for the fact that ablation at strongly absorbed wavelengths is induced without noticeable morphological modifications to the etched substrate (clean etching).<sup>13,14</sup> The same argument can explain the negligible degradation (i.e., for the highly absorbing PS, chemical modifications are limited to the very shallow optical penetration depth ( $\approx 1\text{--}2\text{ }\mu\text{m}$ )), and the degradation is further reduced via the etching process.

**Femtosecond Irradiation.** Upon irradiation of PMMA at 248 nm with 500 fs pulses at fluences higher than the ablation threshold (lower than  $100\text{ mJ/cm}^2$ , as determined by profilometric measurements), no significant changes are observed in the spectra: there are neither new bands nor changes in intensity or position of the bands, showing no dependence on the polymer  $M_w$ . Although the effective optical penetration depth for the doped PMMA films is lower (around  $2\text{ }\mu\text{m}$ ) than the one determined upon nanosecond irradiation (as listed in Table 1), the affected layer is thick enough to be adequately measured by the Raman microprobe. These results indicate that, within the experimental detection limit, irradiation with 248 nm and 500 fs pulses does not induce formation of  $\text{C}=\text{C}$  or other degradation products.

## Discussion

Raman examination shows a significant dependence of the effects induced on doped polymers upon nanosecond laser irradiation on the polymer  $M_w$  and on the absorption coefficient of the system at the irradiation wavelength. In the case of doped PMMA irradiated with a KrF laser, the main effects induced are the increase of intensity of the band at  $1640\text{ cm}^{-1}$  assigned to  $\nu(\text{C}=\text{C})$  and the appearance of new bands in the region of  $1700\text{--}1800\text{ cm}^{-1}$ , which typically corresponds to  $\nu(\text{C}=\text{O})$ .

The increase of intensity of the  $\nu(\text{C}=\text{C})$  band indicates the creation of unsaturation or reactive centers resulting from hydrogen-atom abstraction from the polymer chain by the

radicals created in the photodissociation of the dopant.<sup>26–31</sup> Another contribution to this band is the photolysis of methyl side chains or ester side groups of the polymer.<sup>5,36</sup> The new bands in the region of  $1700\text{--}1800\text{ cm}^{-1}$  are assigned to degradation products containing in their structure the  $\text{C}=\text{O}$  bond.

The slight increase of effects observed for the irradiation with successive pulses is a typical sign for incubation. The phenomenon of incubation, in which under repetitive irradiation, ablation begins below the single pulse ablation threshold, occurs in materials with low absorption coefficient at the laser wavelength. For irradiation of PMMA, at wavelengths longer than 193 nm, incubation effects are known to be particularly pronounced<sup>16,37–41</sup>. A permanent increase in absorptivity after UV irradiation of PMMA due to chemical changes in the polymer is well-established.<sup>40</sup>

Characterization of the effects of UV irradiation of pure PMMA has been extensively studied<sup>5,15,36,37,42–44</sup>. Three main effects have been proposed: (1) random homolytic scission of the polymer backbone producing carbon radicals that can initiate unzipping reactions (depolymerization), (2) photolysis of the methyl side chain, producing chain end  $\text{C}=\text{C}$  double bonds and radicals, which can again initiate polymer unzipping, and (3) photolysis of the ester side group. The latter is the most important reaction at wavelengths longer than 230 nm.<sup>37</sup> Using picosecond ionization of the ejecta, Stuke showed that the polymeric ejected species must be unsaturated fragments containing the  $\text{C}=\text{C}$  bond.<sup>45</sup> This has been confirmed by mass-spectrometric studies by Krajnovich.<sup>46</sup> FTIR analyses have indicated that similar species are formed in the substrate.<sup>16</sup> In fact, in laser induced fluorescence examination of the irradiated neat PMMA and ArI-doped PMMA, Andreou et al.<sup>31</sup> have observed, both below and above the ablation threshold, a broad emission band at  $\approx 400\text{--}450\text{ nm}$  that grows with successive laser pulses; this band can be assigned to conjugated structures containing  $\text{C}=\text{C}$ . These results are in good agreement with those reported here.

As reported by several authors, photolysis of the ester side group often yields small radicals such as the methoxy, methyl, and methyl formate radicals<sup>36,37,42,43</sup> as shown in Figure 3a. These radicals can abstract hydrogen from the remainder of the chain to form  $\text{CH}_3\text{OH}$ ,  $\text{CH}_4$ , and  $\text{HCOOCH}_3$ . Hydrogen-atom abstraction from the polymer also produces main chain double bonds, which enhance laser absorption and provide vulnerable sites for the initiation of thermal unzipping. A variety of experiments has confirmed that PMMA photolysis at wavelengths longer than 240 nm generates gaseous molecules ( $\text{CH}_3\text{OH}$ ,  $\text{CH}_4$ ,  $\text{HCOOCH}_3$ ,  $\text{CO}$ , and  $\text{CO}_2$ , see Figure 3a) and that the associated chain radicals quickly react with small radicals.<sup>44</sup> FTIR spectroscopy has also revealed the presence of the aldehyde ( $\text{H}_2\text{--C}=\text{O}$ ) product.<sup>44</sup>

Thermal unzipping of PMMA yields the monomer methylacrylate (MMA) as shown in Figure 3b. In the case of the doped systems actually studied here, the thermal decomposition/unzipping process dominates.<sup>27</sup> Furthermore, already at low enough fluences ( $\geq 200\text{ mJ/cm}^2$ ), high enough temperatures are developed at relatively low fluences, as a result of the increasing importance of nonlinear/multiphoton absorption processes. Multiphoton processes have been demonstrated in the irradiation at 248 nm of PMMA with a variety of dopants.<sup>47–49</sup> Since the absorption coefficient is independent of the PMMA  $M_w$ , a direct photolytic process cannot explain why polymer decomposition should vary with  $M_w$ . Instead, as discussed next, the thermal decomposition process can rather directly account for this dependence.

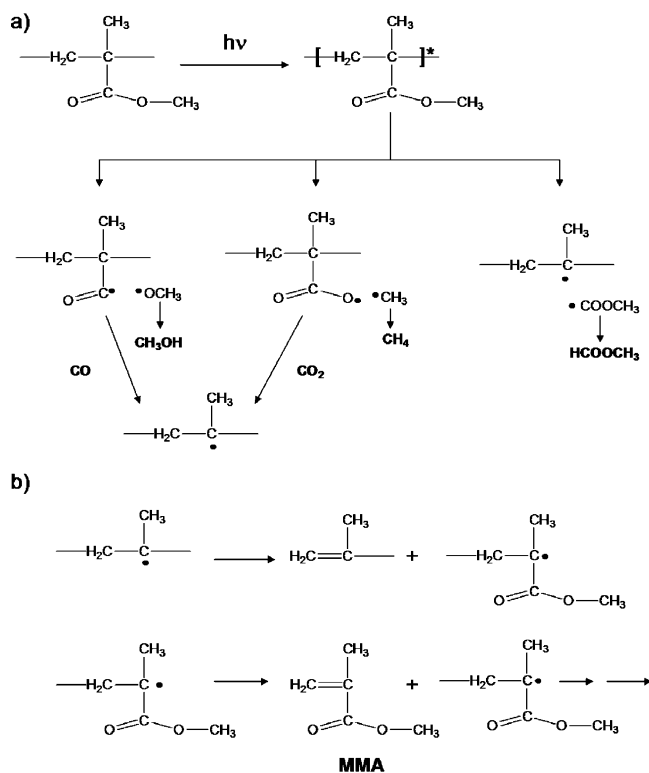


**Figure 3.** Degradation scheme of PMMA upon KrF irradiation: (a) photolysis of the ester side chain and (b) double-bond formation and decomposition of PMMA giving rise to the monomer MMA.

According to the results that we present here, at irradiation fluences below the ablation threshold, the main effect induced in PMMA is the formation of the C=C bond as a consequence of the degradation of the polymer. Expectably, upon irradiation at higher fluences, effects are more pronounced, and the formation of additional products is observed together with the C=C bond formation. Most importantly, for larger  $M_W$  systems, the previous changes are clearly more pronounced (demonstrating that polymer degradation is much more extensive for the higher  $M_W$ ). These Raman results correlate well with laser induced fluorescence measurements to be described elsewhere,<sup>50</sup> probing a dopant-deriving product (i.e., NapH and PhenH for NapI- and PhenI-doped PMMA, respectively) formation. These studies find that at fluences  $>250$  mJ/cm<sup>2</sup>, ArH formation is increasingly higher in the high  $M_W$  system than in the low  $M_W$ . Because ArH is formed via a simple thermal-activated reaction (i.e., hydrogen-atom abstraction from the polymer<sup>27</sup>), this result demonstrates that higher temperatures are attained in the high  $M_W$  PMMA. This finding directly also accounts for the higher extent of thermal decomposition of the polymer itself observed by the Raman results. The higher extent of decomposition for the high  $M_W$  is also demonstrated by the fact that below the ablation threshold, although swelling is observed for all systems,<sup>13</sup> it is much more pronounced for the higher  $M_W$  system (e.g., for 1.2% NapI/PMMA, the maximum swelling is 8  $\mu$ m vs 4  $\mu$ m for the low  $M_W$  polymer).

As discussed in detail elsewhere,<sup>50</sup> the previous difference in the attained temperatures can be largely explained within a thermal model of the interaction of 248 nm irradiation with PMMA. Briefly, for thermal decomposition, a much higher number of bonds has to be broken in the higher  $M_W$  systems for chain decomposition into monomers/oligomers that can desorb in the gas phase. For the low  $M_W$  PMMA, decomposition of the polymer in gaseous monomers is comparatively efficient; it is estimated to be significant at fluences as low as 250 mJ/

cm<sup>2</sup>. As a result of the efficient desorption of gaseous species and thus energy removal, much lower temperatures are attained in the low  $M_W$  system. On the other hand, for the higher  $M_W$ , monomer formation and energy removal is much reduced or negligible, thus accounting for the much higher temperatures attained (at the same fluence). Furthermore, according to a thermal mechanism (more precisely, within the bulk photothermal model<sup>21,22</sup>), the ablation threshold and the etching rate are specified by the condition that a critical fraction of bonds is broken at the interface. Clearly, the model implies that a critical concentration of monomers/oligomers is reached at the surface. For low  $M_W$ , this critical concentration is attained at relatively low laser fluences/temperatures, resulting in a low ablation threshold (as shown in Table 1). In contrast, in the high  $M_W$  systems, because of the necessity of dissociating a much higher number of bonds, their ablation takes place at much higher fluences/temperatures. Thus, not only higher temperatures are attained in the high  $M_W$  system but also ablation occurs at higher fluences (i.e., an even higher temperature difference). The examination of the ArH formation kinetics<sup>50</sup> allows the estimation of the surface temperatures at the corresponding ablation thresholds, which are  $\sim 800$  K for  $M_W \geq 120$  kDa versus  $\sim 600$  K for the 1.9 kDa PMMA. Therefore, this difference in the attained temperatures can account for the higher extent of polymer decomposition observed in the substrate of the higher  $M_W$  PMMA.

For doped PS, no significant changes are induced upon irradiation at 248 nm. At this wavelength, PS is a highly absorbing system,<sup>13,14</sup> and the optical penetration depth is very much reduced, finally resulting in a significantly less amount of material affected by the laser irradiation. This would explain why degradation products are not observed. In fact, by microscopic and profilometric examinations of the irradiated areas, no morphological modifications were detected. As mentioned previously, no effects were detected for any of the polymer  $M_W$  employed. This can be due to the fact that if any, changes must be too small to be observed.

In the case of irradiation of doped PMMA at 248 nm with 500 fs pulses, effects are not induced in the irradiated areas nor is dependence on polymer  $M_W$  observed. These results agree well with those obtained by other techniques<sup>51</sup> and suggest that the mechanisms involved in the femtosecond laser ablation differ from the mechanisms that operate in the case of nanosecond laser ablation. The independence of the results from the polymer  $M_W$  indicates that simple decomposition of the polymer to the constituent monomers is not involved; otherwise, pronounced differences would be observed as in the case of nanosecond ablation. Mechanisms operating in femtosecond laser ablation are typically discussed in terms of the formation of a weak plasma within the substrate as a result of multiphoton and subsequent avalanche processes.<sup>52</sup> The laser energy is deposited into free, or quasi-free, electrons that are produced by the previous processes, rather than in the bulk material, and is transferred into kinetic energy of the ablation products.

## Conclusion

We have examined the influence of  $M_W$  on the chemical modifications induced upon UV laser ablation of PMMA and PS films doped with active iodo-substituted derivatives, via micro-Raman spectroscopic characterization of the irradiated substrates. Raman spectra reveal that  $M_W$  has a strong influence on the chemical effects induced upon ablation for low absorbing polymer films. The results provide direct support for the bulk photothermal model, according to which ejection requires that

a critical number of bonds are broken. In the case of irradiation with a hybrid excimer-dye laser with a pulse duration of 500 fs, mechanisms involved differ from those operating in the case of nanosecond laser ablation, and participation of multiphoton/avalanche processes is suggested.

**Acknowledgment.** Funding from MCYT (Project BQU2003-08531-C02-01) is gratefully acknowledged. M.O. and E.R. thank CSIC I3P for a contract and a fellowship, respectively. Collaboration has also been possible by funding from the Ultraviolet Laser Facility operating at FO.R.T.H. under the Improving Human Potential (IHP)-Access to Research Infrastructures program (RII3-CT-2003-506350) and the ESF COST Action G7.

## References and Notes

- (1) *Advances in polymer science, polymers, and light*; Lippert, T., Ed.; Springer-Verlag: Berlin, 2004.
- (2) *Photochemical processing of electronic materials*; Boyd, I. A., Ed.; Academic Press: London, 1992.
- (3) Bäuerle, D. *Laser processing and chemistry*; Springer-Verlag: Berlin, 2000.
- (4) Vogel, A.; Venugopalan, V. *Chem. Rev.* **2003**, *103*, 577.
- (5) Lippert, T.; Dickinson, T. *Chem. Rev.* **2003**, *103*, 453.
- (6) Preuss, S.; Spath, M.; Zhang, Y.; Stuke, M. *Appl. Phys. Lett.* **1993**, *62*, 3049.
- (7) König, K.; Riemann, I.; Fritsche, W. *Opt. Lett.* **2001**, *26*, 819.
- (8) Baudach, S.; Krüger, J.; Kautek, W. *Rev. Laser Eng.* **2001**, *29*, 705.
- (9) Lemoine, P.; Blau, W.; Drury, A. *Polymer* **1993**, *34*, 5020.
- (10) Lippert, T.; Stebani, J.; Ihlemann, J.; Nuyken, O.; Wokaun, A. *Angew. Makromol. Chem.* **1993**, *213*, 127.
- (11) Mito, T.; Masuhara, H. *Appl. Surf. Sci.* **2002**, *197–198*, 796.
- (12) Rebollar, E.; Bounos, G.; Oujja, M.; Domingo, C.; Georgiou, S.; Castillejo, M. *Appl. Surf. Sci.* **2005**, *248*, 254.
- (13) Rebollar, E.; Bounos, G.; Oujja, M.; Georgiou, S.; Castillejo, M. *J. Phys. D: Conf. Ser.*, in press.
- (14) Rebollar, E.; Bounos, G.; Oujja, M.; Georgiou, S.; Castillejo, M. *J. Phys. Chem. B*, submitted for publication.
- (15) Beauvois, S.; Renaut, D.; Lazzaroni, R.; Laude, L. D.; Bredas, J. G. L. *Appl. Surf. Sci.* **1997**, *109–110*, 218.
- (16) Küper, S.; Stuke, M. *Appl. Phys. A* **1989**, *49*, 211.
- (17) Rossier, J. S.; Bercier, P.; Schwarz, A.; Lorient, S.; Girault, H. *Langmuir* **1999**, *15*, 5173.
- (18) Lippert, T.; Ortelli, E.; Panitz, J.-C.; Raimondi, F.; Wambach, J.; Wei, J.; Wokaun, A. *Appl. Phys. A* **1999**, *69*, S651.
- (19) Dyer, P. E.; Pervolaraki, M.; Lippert, T. *Appl. Phys. A* **2005**, *80*, 529.
- (20) Lazare, S.; Lopez, J.; Turlet, J.-M.; Kufner, M.; Kufner, S.; Chavel, P. *Appl. Opt.* **1996**, *35*, 4471.
- (21) Bityurin, N.; Luk'yanchuk, B. S.; Hong, M. H.; Chong, C. T. *Chem. Rev.* **2003**, *103*, 519.
- (22) Arnold, N.; Bityurin, N. *Appl. Phys. A* **1999**, *68*, 615.
- (23) Willis, H. A.; Zichy, V. J. I.; Hendra, P. J. *Polymer* **1969**, *10*, 737.
- (24) Bertoluzza, A.; Fagnano, C.; Monti, P.; Semeraro, G.; García-Ramos, J. V.; Caramazza, R.; Cellini, M. *J. Raman Spectrosc.* **1987**, *18*, 151.
- (25) Socrates, G. *Infrared and Raman characteristic group frequencies. Tables and charts*; John Wiley and Sons: London, 2001.
- (26) Bounos, G.; Athanassiou, A.; Anglos, D.; Georgiou, S. *Chem. Phys. Lett.* **2006**, *418*, 317.
- (27) Bounos, G.; Kolloch, A.; Stergiannakos, T.; Varatsikou, E.; Georgiou, S. *J. Appl. Phys.* **2005**, *98*, 1.
- (28) Lassithiotaki, M.; Athanassiou, A.; Anglos, D.; Georgiou, S.; Fotakis, C. *Appl. Phys. A* **1999**, *69*, 363.
- (29) Bounos, G.; Athanassiou, A.; Anglos, D.; Georgiou, S.; Fotakis, C. *J. Phys. Chem. B* **2004**, *108*, 7052.
- (30) Rebollar, E.; Oujja, M.; Castillejo, M.; Georgiou, S. *Appl. Phys. A* **2004**, *79*, 1357.
- (31) Andreou, E.; Athanassiou, A.; Fragouli, D.; Anglos, D.; Georgiou, S. *Laser Chem.* **2002**, *20*, 1.
- (32) Haselbach, E.; Rohner, Y.; Suppan, P. *Helv. Chim. Acta* **1990**, *73*, 1644.
- (33) Dzvonik, M.; Yang, S.; Bersohn, R. *J. Chem. Phys.* **1974**, *61*, 4408.
- (34) Birks, J. B. *Photophysics of aromatic molecules*; John Wiley and Sons: London, 1970.
- (35) Rebollar, E.; Bounos, G.; Oujja, M.; Kolloch, A.; Georgiou, S.; Castillejo, M. *J. Appl. Phys.*, submitted for publication.
- (36) Wochowski, C.; Metev, S.; Sepold, G. *Appl. Surf. Sci.* **2000**, *154–155*, 706.
- (37) Lippert, T.; Webb, R. L.; Langford, S. C.; Dickinson, J. T. *J. Appl. Phys.* **1999**, *85*, 1838.
- (38) Srinivasan, R.; Braren, B.; Casey, K. G. *Pure Appl. Chem.* **1990**, *62*, 1581.
- (39) Davis, G. M.; Gower, M. C. *J. Appl. Phys.* **1987**, *61*, 2090.
- (40) Meyer, J.; Kutzner, J.; Feldmann, D.; Welge, K. H. *Appl. Phys. B* **1988**, *45*, 7.
- (41) Srinivasan, R.; Braren, B.; Casey, K. G. *J. Appl. Phys.* **1990**, *68*, 1842.
- (42) Wochowski, C.; Shams-el-Din, M. A.; Metev, S. *Polym. Degrad. Stab.* **2005**, *89*, 252.
- (43) Shams-el-Din, M. A.; Wochowski, C.; Metev, S.; Hamza, A. A.; Jüptner, W. *Appl. Surf. Sci.* **2004**, *236*, 31.
- (44) Gupta, A.; Liang, R.; Tsay, F. D.; Moacanin, J. *Macromolecules* **1980**, *13*, 1696.
- (45) R, Larciprete.; Stuke, M. *Appl. Phys. B* **1987**, *42*, 181.
- (46) Krainovich, D. J. *J. Phys. Chem. A* **1997**, *101*, 2033.
- (47) Fujiwara, H.; Nakajima, Y.; Fukumura, H.; Masuhara, H. *J. Phys. Chem.* **1995**, *99*, 11481.
- (48) Furutani, H.; Fukumura, H.; Masuhara, H. *J. Phys. Chem.* **1996**, *100*, 6871.
- (49) Fukumura, H.; Masuhara, H. *Chem. Phys. Lett.* **1994**, *221*, 373.
- (50) Bounos, G.; Rebollar, E.; Selimis, A.; Bityurin, N.; Castillejo, M.; Georgiou, S. *J. Appl. Phys.*, submitted for publication.
- (51) Bounos, G.; Rebollar, E.; Castillejo, M.; Georgiou, S. Manuscript in preparation.
- (52) Vogel, A.; Noack, J.; Hüttmann, G.; Paltauf, G. *Proc. SPIE-Int. Soc. Opt. Eng.* **2002**, *4633*, 23.